DOE/ER/10556-1

COO-3084-79

TECHNICAL PROGRESS REPORT

Contract DE-AC02-80ER10556 A000

"A Combined Macroscopic and Microscopic Approach to the Fracture of Metals"

Annual Progress Report: 1979-1980

R. J. Asaro, J. Gurland, A. Needleman, and J. R. Rice

Division of Engineering

Brown University

Providence, Rhode Island

U. S. Department of Energy

Contract No. DE-AC02-80ER 10556 A000

Technical Report No. 79

June 1980

DISCLAIMER

Summary of Significant Accomplishments

Among the most significant results obtained this past year were the following: 1) Extremely good theoretical-experimental correlation was found between our theoretical predictions based on asymptotic analysis with numerical finite element studies and the experimentally monitored crack growth for a large range of stable crack growth in 4140 steel; 2) A theoretical model was developed for the critical conditions of crack initiation at rigid particles as a precursor of ductile rupture in steels; 3) As part of our study of environmentally sensitive fracture mechanisms, it was found that hydrogen can promote a ductile-to-brittle fracture transition with increasing charging current density in low carbon steel; and 4) A new variational principle has been established for the combined processes of plastic creep flow and grain boundary diffusion and has been constructively applied to the problem of cavity growth under creep conditions.

Table of Contents

A. Detailed Description of Research Program

1. Elastic-Plastic Analysis of Stable Crack Growth
2. Microstructural Aspects of Fracture Processes in Ductile Alloys
   a) Void nucleation in spheroidized steels during tensile deformation.
   b) Fracture initiation and propagation in ductile two-phase alloys.
   c) Correlation of microstructure with fracture toughness in high strength steels.
3. Environmentally Sensitive Fracture Mechanisms
   a) Thermodynamics of interfacial separation
   b) The role of hydrogen in medium strength steels.
   c) Hydrogen assisted fractures in high strength steels.
4. Elevated Temperature Rupture Processes
   a) Processes of diffusive cavitation, including combined effects of plastic creep flow and diffusion.
   b) Diffusive alleviation of transient stress concentrations.
   c) Creep effects in macro-crack growth.

Table of Contents (continued)

B. Reports, Publications, Theses, Oral Presentations and Other Related Activities

1. Technical Reports

2. Publications

3. Theses

4. Oral Presentations and Seminars

C. Personnel

1. Personnel Connected with Contract

A. DETAILED DESCRIPTION OF RESEARCH PROGRAM

1. Elastic-Plastic Analysis of Stable Crack Growth

Our work on the study of elastic-plastic crack growth in ductile metals includes analytical and finite element studies which are closely coordinated with experimentation. Recent efforts have been directed toward filling-in and extending the theoretical framework provided by Rice, Drugan and Sham (Technical Report No. 65) for describing stable crack growth, and especially toward study of the experimental validity of the predictions made. As summarized in the last Progress Report, the Rice, Drugan and Sham study combined an asymptotic analysis with numerical finite element studies to determine the stress and deformation fields very near the tip of a growing crack in an elastic-ideally plastic material. This knowledge was then coupled with a fracture criterion, based on a self-similar deformation state near the crack tip during growth, to yield a fairly complete description of stable crack growth in elastic-ideally plastic solids under small scale yielding conditions.

Further details of the elastic-ideally plastic asymptotic crack tip analysis, of which only the major results were presented in the Rice, Drugan and Sham report, have been written-up and will be submitted for publication by Drugan and Rice. This work includes discussion of conditions for validity and uniqueness of the near-tip field, as well as of three-dimensional effects entering the Mises yield criterion and flow rule near the crack tip.

Analytical work is continuing to extend these results for the elastic-ideally plastic model to conditions of crack growth under large scale yielding and fully plastic conditions. The determination of near tip fields for cracks growing in strain hardening materials of the type $\sigma \propto \varepsilon^N$ is also

under study. Here, we have been able to rule out the possibility of power-like behavior of stress and strain on distance from the tip, of the form known to result from the Hutchinson-Rice-Rosengren solutions for a stationary crack. However, we have not yet been able to determine the appropriate type of singularity. Encouragement for and insight into such theoretical investigations have been provided by the recent experimental results of Hermann and Rice (Technical Report No. 76) on an AISI 4140 steel, to be discussed later in this section, which suggest remarkably good agreement with theoretical predictions from the Rice, Drugan and Sham contained yielding results.

Work on a final finite element solution for a stably growing crack in an elastic-ideally plastic solid under small scale yielding and plane strain conditions is continued. The goal is to correlate the finite element solution with the crack opening rate,

$$\dot{\delta} = \alpha \dot{J}/\sigma_o + \beta (\sigma_o/E) \dot{a} \ell n (R/r) \qquad \text{as } r \to 0 ,$$

obtained from the asymptotic analysis, in an effort to identify the parameters α and R (which are undetermined in the asymptotic analysis) definitively, and to determine their dependence on the J-integral and the crack growth history. These parameters are critical since the crack growth criterion of Rice, Drugan and Sham is based on an integrated and rephrased version of this expression. (This criterion requires a geometrically similar crack tip shape for continued growth.) In the above equation, $\dot{\delta}$ is the rate of crack opening at small distances r behind the crack tip, J is the far field value of the J-integral, σ_o is the ideally plastic yield strength in simple tension, E is Young's modulus, a is the crack length and $\beta = 5.08$ (for Poisson ratio of 0.3). In addition, the plastic strain obtained from the asymptotic analysis

is given as

$$\varepsilon_{ij}^{p} = \frac{2-\nu}{\sqrt{6}} \frac{\sigma_o}{E} G_{ij}(\theta) \ln\left(\frac{\bar{R}}{r}\right) + H_{ij}(\theta) , \qquad \text{as } r \to 0 ,$$

where the $G_{ij}(\theta)$ are known functions (Technical Report No. 65) but where $\bar{R}$, which is related to R, and $H_{ij}(\theta)$ are undetermined by the asymptotic analysis; however, $H_{ij}(\theta)$ will depend, in a presumably monotonically increasing manner, on the ratio d(applied load)/da. We have noted previously that an alternative fracture criterion can be based on the intensity of accumulated plastic strain near the tip. Therefore, we also want to correlate the finite element solution with this asymptotic relation to determine $H_{ij}(\theta)$ and $\bar{R}$, and other features of the strain distribution. Certain numerical inaccuracies were detected in the finite element solution, based on a highly-refined mesh, obtained previously (Sham, ScM thesis, 1979); hence there were ambiguities in determining the parameters α and R from this solution.

In the Sham solution, a boundary layer formulation is employed to analyze this problem of plane strain crack growth under small scale yielding conditions; namely, the elastic crack singularity is used to set the far-field displacement boundary conditions on this elastic-plastic boundary valve problem:

$$\underset{\sim}{u} \to (K/2E) \sqrt{r}\, \underset{\sim}{F}(\theta) \qquad \text{as } r \to \infty$$

where K is the stress intensity factor and $\underset{\sim}{F}(\theta)$ is a normalized tensor describing the angular displacement variations. The assumption of small scale yielding conditions imposes the requirement on mesh design that the outermost radius of the mesh must be much greater than the maximum plastic zone extent, r_p. On the other hand, we must correlate the finite element results with the asymptotic analysis to estimate the aforementioned undetermined parameters α and R, which requires the distance from the tip to

the node at which numerical data are sampled to be much less than r_p in order to simulate asymptotic conditions. Further, since success has not yet been realized in developing crack tip singular elements which incorporate the correct singularity for a growing crack, a very refined mesh must be employed near the crack tip to accommodate the high strain gradients there; even so, the method is highly taxed near the tip, so that accurate representation of the stress and strain fields cannot be expected closer than 5 to 6 elements from the crack tip. Hence, to achieve high accuracy with such a formulation, all of these requirements must be well-satisfied, requiring an enormous number of nodes.

In view of these difficulties, an alternative finite element formulation has been developed. Let Γ_R be a circular arc centered at the crack tip of sufficient radius R that the plastic region is always contained within it, as shown in Fig. 1.1. Denote the region outside Γ_R as A_E and the region inside Γ_R as A_P. The displacements

$$\underset{\sim}{u} = (K/2E)\, r^{1/2}\, \underset{\sim}{F}(\theta)$$

corresponding to the elastic K field are prescribed along Γ (where, ultimately, the radius of Γ is made infinite) and traction-free boundary conditions are prescribed on the crack surface. Following Rice (J. Mech. Phys. Solids, 1974), we utilize a version of the "Williams expansion" (M. L. Williams, J. Appl. Mech., 1957) of the stress and displacement field, which is convergent in the outer rather than inner field, for this outer region A_E, to arrive at the representations

$$\underset{\sim}{\sigma} = K\, r^{-1/2}\, \underset{\sim}{f}(\theta) + C_1\, r^{-3/2}\, \underset{\sim}{g}(\theta) + C_2\, r^{-2}\, \underset{\sim}{h}(\theta) + \ldots$$

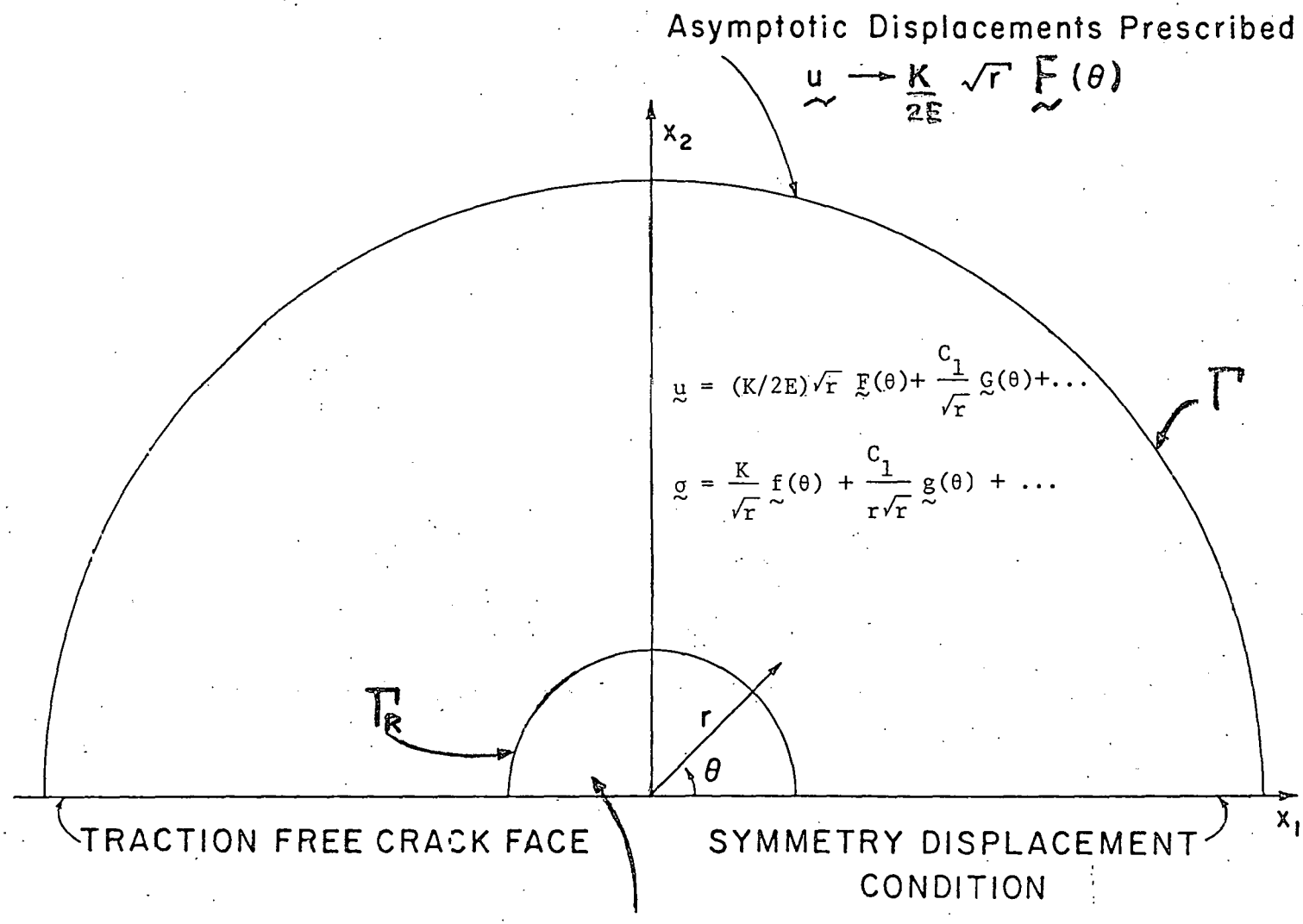
Asymptotic Displacements Prescribed
$\underset{\sim}{u} \rightarrow \frac{K}{2E}\sqrt{r}\,\underset{\sim}{F}(\theta)$
x_2
$\underset{\sim}{u} = (K/2E)\sqrt{r}\,\underset{\sim}{F}(\theta) + \frac{C_1}{\sqrt{r}}\underset{\sim}{G}(\theta) + \ldots$
$\underset{\sim}{\sigma} = \frac{K}{\sqrt{r}}\underset{\sim}{f}(\theta) + \frac{C_1}{r\sqrt{r}}\underset{\sim}{g}(\theta) + \ldots$
Γ
Γ_R
r
θ
x_1
TRACTION FREE CRACK FACE
SYMMETRY DISPLACEMENT CONDITION
FINITE ELEMENT MESH

Figure 1.1

$$\underset{\sim}{u} = (K/2E)\, r^{1/2}\, \underset{\sim}{F}(\theta) + C_1\, r^{-1/2}\, \underset{\sim}{G}(\theta) + C_2\, r^{-1}\, \underset{\sim}{H}(\theta) + \ldots$$

Here, r and θ are the polar coordinates centered at the crack tip, the functions of angle θ are known and the coefficients, C_i, $(i = 1,2,\ldots)$, are unknown. The potential energy of region A_E can then be expressed in terms of these coefficients. As for the region A_p, it is discretized into finite elements in the usual manner and we take the nodal displacements along Γ_R to be those given by the Williams expansion. Hence, the potential energy (or equivalent functional, for elastic-plastic response) for this region can be calculated in terms of the unknown nodal displacements inside A_p (not including those on Γ_R) and the unknown coefficients. Thus the total potential energy of the entire region (A_E and A_p) can be obtained readily as the sum of the two. This total potential energy is then minimized with respect to the unknown coefficients (noting that K is regarded as a known quantity) and the nodal displacements, and this leads to two sets of finite element equilibrium equations with two sets of unknowns; namely, the nodal displacements inside A_p and the unknown coefficients. After eliminating the unknown coefficients, there remains one set of finite element equilibrium equations with the nodal displacements inside A_p as unknowns to be determined by usual finite element procedures.

By using this procedure, the small scale yielding condition is always satisfied even if the plastic zone grows near to Γ_R since we can consider the boundary Γ on which displacements are prescribed to be at infinity mathematically. So all available nodal degrees of freedom can be concentrated inside A_p, and by doing so we can capture the state of stress and strain very near the crack tip much more accurately. The implementation of

this procedure into the finite element program is underway.

Another discrepancy detected in the previously obtained finite element solution was that the constant strain triangles, conformed to quadrilaterals to relieve artificial mesh constraints, did not respond favorably during elastic unloading. Isolated groups of elastic elements were found embedded in oceans of yielded elements. To remedy this, a 4-noded isoparametric quadrilateral is used in conjunction with a revised variational principle given by Nagtegaal et al. (Comp. Meth. Appl. Mech. Engr., 1974) in the new calculation. A new mesh with 4-noded isoparametric quadrilaterals has been designed in accordance with the conditions on the mesh design as discussed above.

Another problem in the numerical finite element work, on which we have recently begun, is the generation of a stable crack growth solution which progresses from small scale yielding to general yield conditions for the geometry of the bend specimen, still within the elastic-ideally plastic model. Such results are critical in extending the theoretical description of stable crack growth to large scale yielding and general yielding configurations, since to apply the theoretical growth equation the parameters α and R must be determined by correlating the finite element solution to the expression for crack opening rate from the asymptotic solution. Further, the geometry and mode of loading correspond closely to the specimens being tested experimentally in our program. Hence, to apply the theoretical growth equation for an arbitrary extent of yielding, we must determine, by such correlation with a finite element solution which encompasses stable crack growth from small scale yielding up through general yield conditions, the precise manner in which α and R depend upon extent of yielding. At present this work is in the stage of mesh design only, and is being done by

an upper level undergraduate (S. Tse) under the direction of Sham and Rice.

Important progress has been made in experimentation carried out specifically to permit assessment of our theoretical predictions for stable crack growth. Hermann and Rice (Technical Report No. 76) extended the work of Odegaard and Asaro by testing the high strength 4140 steel studied earlier (Technical Reports Nos. 66 and 67), heat treated to a relatively ductile condition. The heat treatment resulted, though, in significant stable crack growth before conditions of general yielding were met. This was done because the theoretical background is well developed at present only for crack growth with well-contained yielding. Four pre-fatigued compact tension specimens were employed. The load P and the opening displacement Δ along the load line were continuously recorded, and a highly accurate differential compliance technique was utilized to measure amounts of stable crack growth (Technical Report 67). The precision of this differential compliance method, which uses low noise, high-gain electronic instrumentation amplifiers to process P-Δ records, is made possible by several improvements developed here to minimize friction and hence hysteresis during the incremental unloading and reloading processes. The loading pins are mounted in needle bearings, and the maximum utility of these bearings over the full range of the test--which includes extensive rotation of the specimen arms due to the large amount of crack growth and deformation--is realized by hanger plates specifically designed to flex as loading increases to accommodate the unavoidable flexure of the loading pins, thus keeping the bearing surfaces parallel to the loading pins. The technique enables resolution of inferred changes in crack size of the order of 0.01 mm, and comparison of <u>total</u> compliance-estimated growth with visually observed growth at the end of each test showed a difference of less than 7% in the worst case. Each test monitored crack growth from the small scale yielding range up

through the general yielding configuration, representing a substantial amount of stable crack growth.

In order to compare the results obtained from these experiments with our theoretical predictions, curves showing the experimentally-determined dependence of the "deformation theory" value of the J-integral, J_d, on crack length a were plotted for each specimen. Here, the current value of J_d is obtained by integrating

$$dJ_d = (2/b)Md\theta - (J_d/b)da$$

$$= (2/b)Pd\Delta - (J_d/b)da$$

throughout the test, having started at $J_d = 0$ when $\Delta = 0$. (Here b is the ligament length, M is the applied moment and $d\theta$ is the increment in rotation). These curves are compared to the theoretical curves of J_d versus crack length a predicted by integrating the expression for $\frac{dJ}{da}$ resulting from the small-scale yielding theory of Rice, Drugan and Sham (wherein it is assumed that a fixed deformation state prevails very close to the tip of a growing crack), namely

$$dJ/da = (\beta/\alpha)(\sigma_o^2/E)\ell n(\rho/eR)$$

where

$$\alpha \approx 0.65$$

and

$$R \approx 0.23\ EJ/\sigma_o^2\ ,$$

as suggested by the numerical finite element solution for small scale yielding; where E, J, σ_o and β are as defined earlier, and $e = 2.718$ is the natural logarithm base.

The above theoretical expressions are based on the elastic-ideally plastic material model; in specifying these theoretical results to the metal tested, approximate account of strain hardening was made by identifying σ_o in the equation for dJ/da as the ultimate (nominal) tensile strength (although in the expression for R, σ_o is taken to be the actual yield stress, since R is related to the size of the plastic zone).

The single free parameter in the theoretical analysis is ρ, which completely governs the form of the near-tip crack profile. This is theorized to be a material parameter, and hence when attempting to correlate the experimental and theoretical results, ρ is chosen to provide the best fit of the theoretical curves to the experimental ones. Notice that the determination of ρ permits theoretical prediction of the value of J necessary for continuing crack growth without further increase in J, denoted $(J)_{ss}$ (for "steady state"). This happens when $R = \rho/e$, which makes $dJ/da = 0$ as evident from the above equation; so

$$(J)_{ss} = 1.60\ \sigma_o^2 \rho/E\ .$$

Figure 1.2 shows the comparison between the experimental J_d versus a curve, denoted by circular symbols, and the theoretically predicted curve (with judicious choice of the free parameter ρ), for each of the specimens tested. The solid curves in Figs. 1.2 (a) to 1.2 (c) (specimens 1 to 3) are identical to the best-fit curve in Fig. 1.2 (d). The value of ρ which generates this curve is $\rho = 7.175$ mm, implying that $(J_d)_{ss} = 80$ kN/M. The dashed curves in Figs. 1.2 (a) to 1.2 (c) are for slightly different ρ values, giving the best fit for each specimen, although the theory implies, of course, that ρ is a specimen-independent material property. The curves

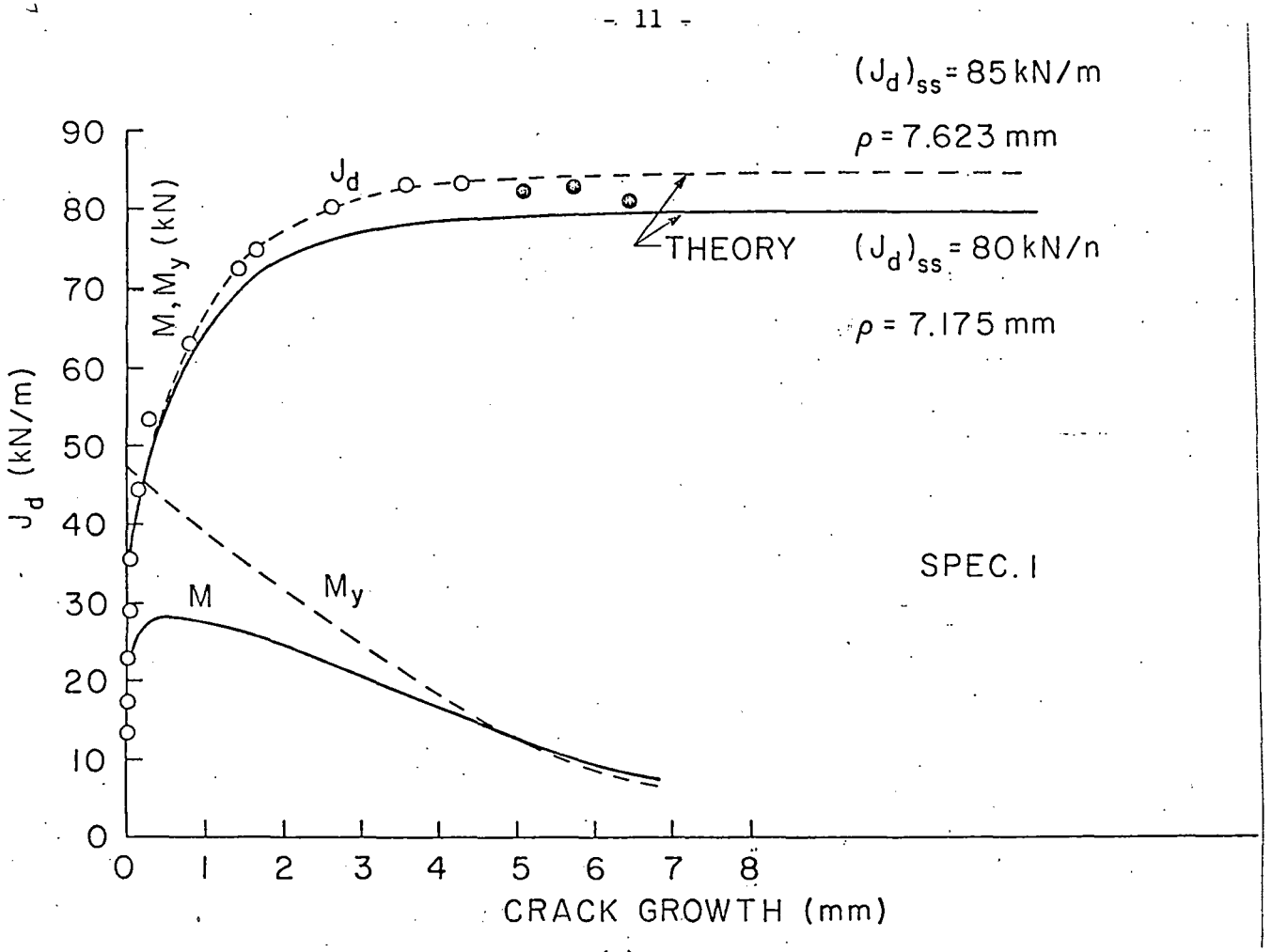
$(J_d)_{ss}$ = 85 kN/m
ρ = 7.623 mm
J_d
THEORY
$(J_d)_{ss}$ = 80 kN/n
ρ = 7.175 mm
M, M_y (kN)
J_d (kN/m)
SPEC. 1
M
M_y
CRACK GROWTH (mm)

(a)

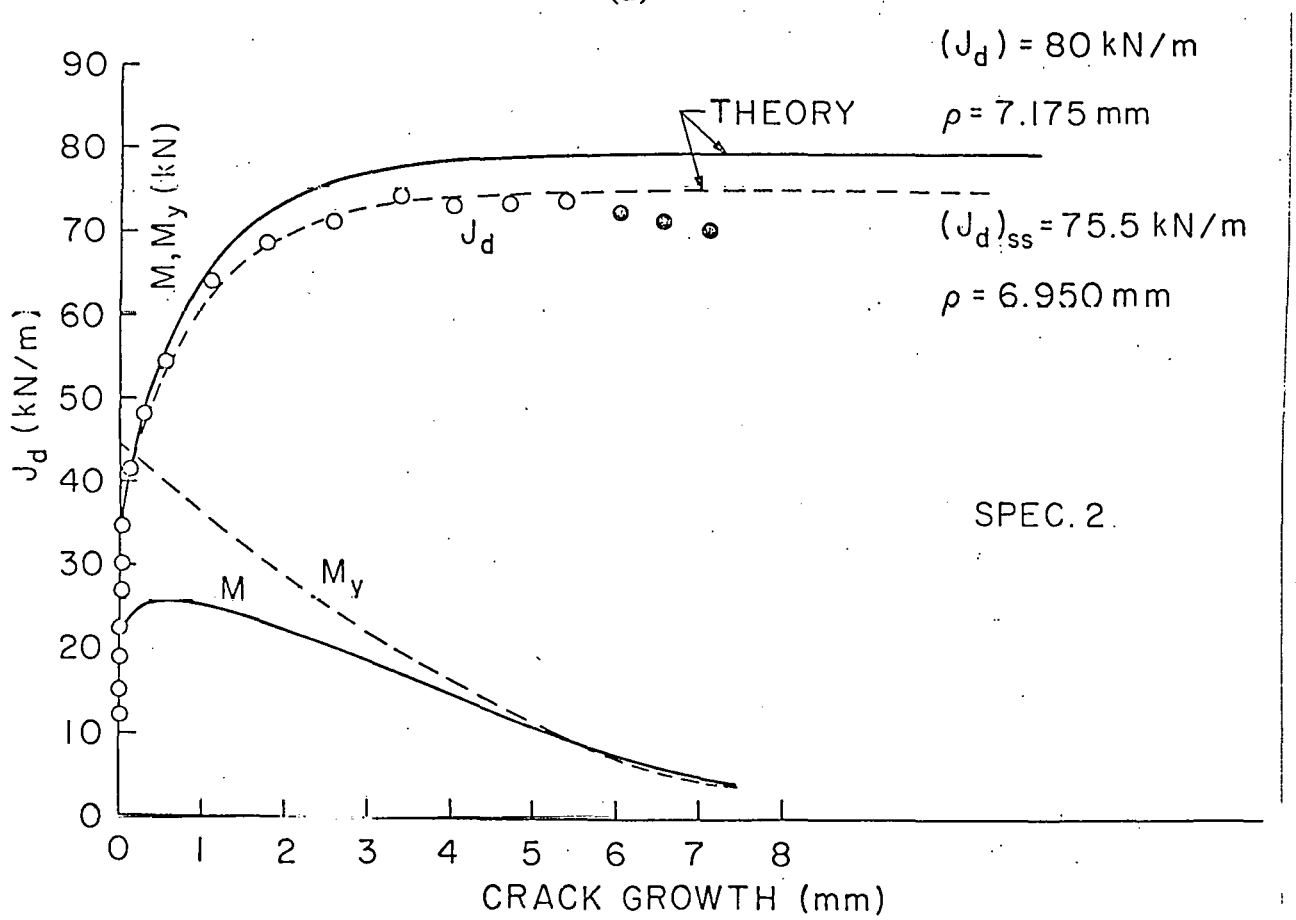
(J_d) = 80 kN/m
THEORY
ρ = 7.175 mm
$(J_d)_{ss}$ = 75.5 kN/m
ρ = 6.950 mm
J_d
M, M_y (kN)
J_d (kN/m)
SPEC. 2
M
M_y
CRACK GROWTH (mm)

(b)

Figure 1.2

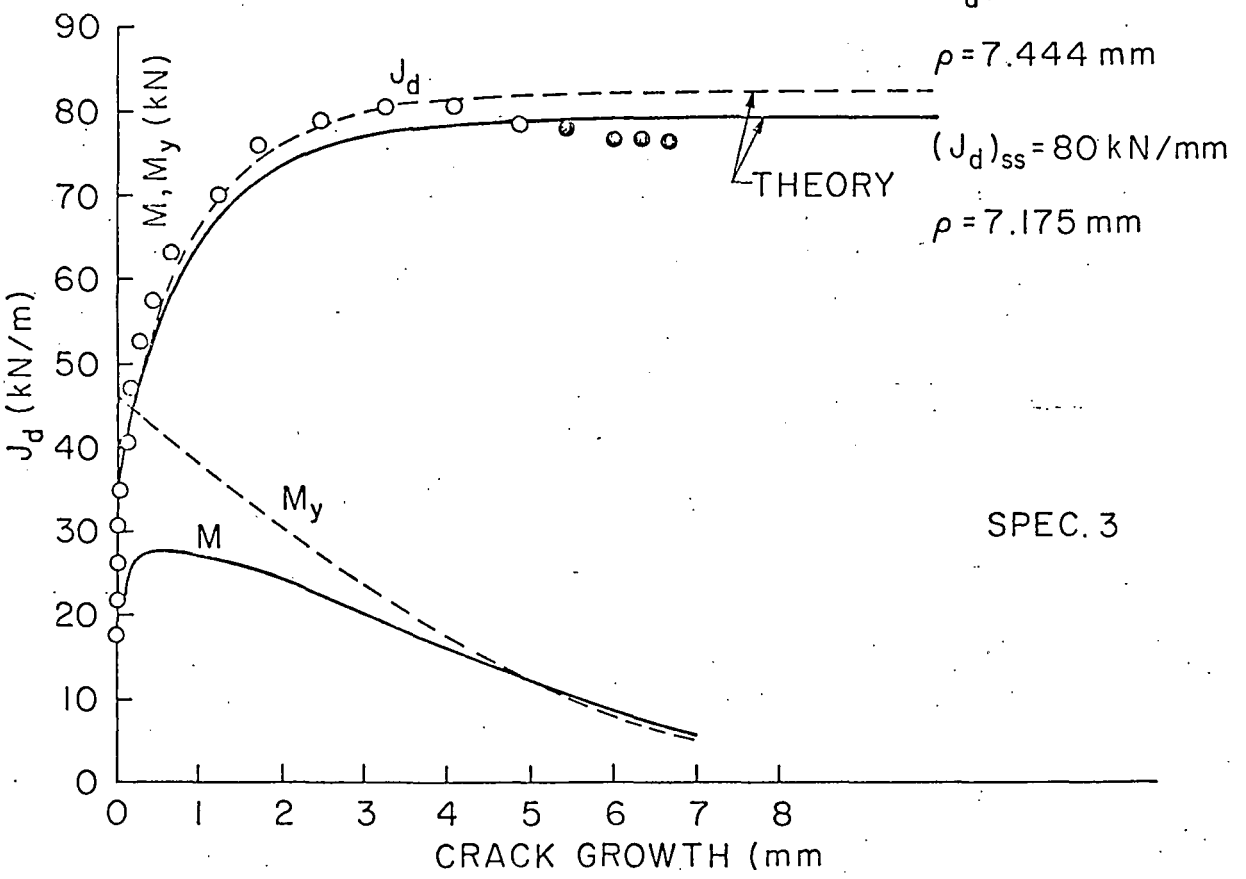

/(c)

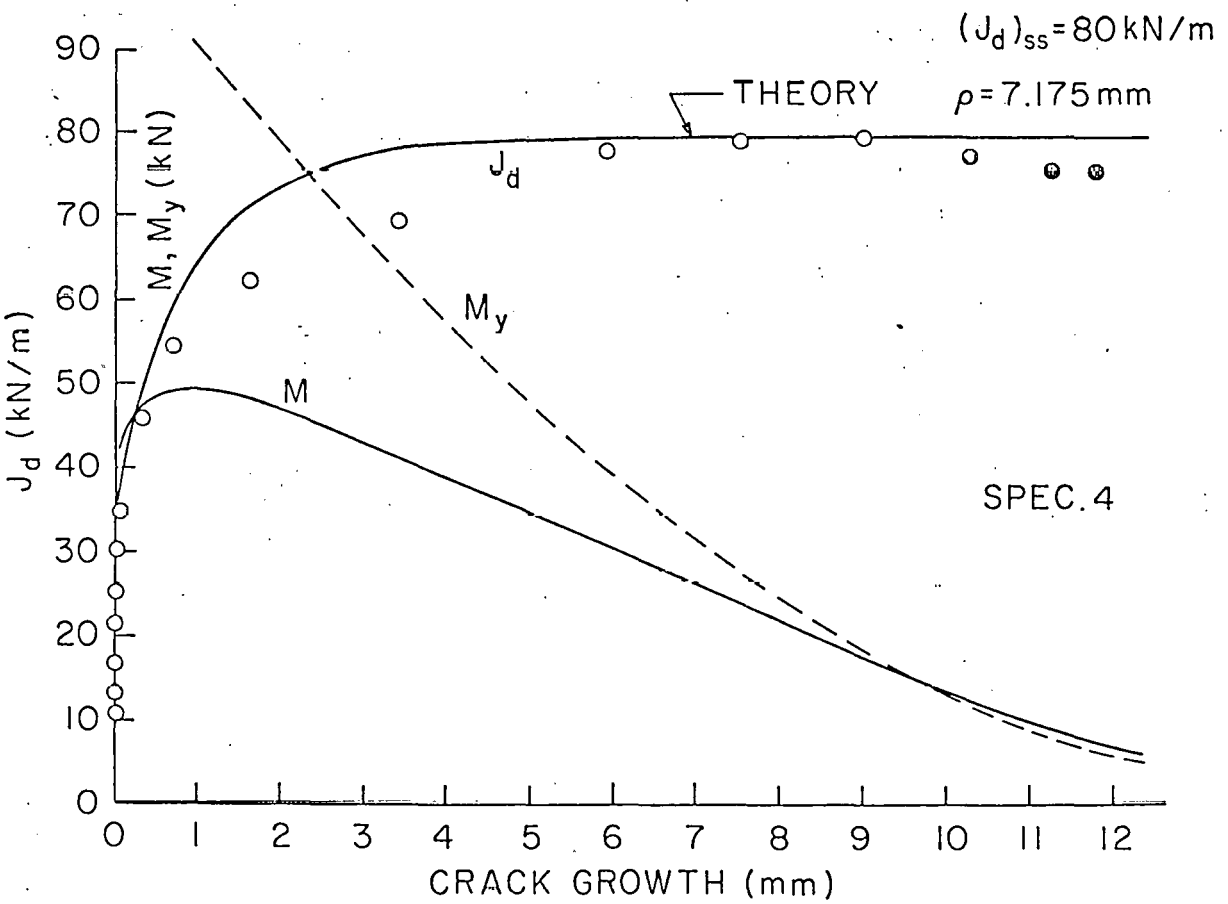

(d)

Figure 1.2 (continued)

labeled M and M_y denote the applied moment and the fully plastic moment, respectively; their comparison shows the early part of the test to correspond to contained yielding, and the later to general yielding. As is evident, extremely good theoretical-experimental correlation is found, for a large range of stable crack growth, and even roughly into the general yielding range (denoted by filled-in circles).

Further experiments on stable crack growth are already underway, directed now by the experimental results just described, in addition to the theoretical framework. One question left open by the Hermann and Rice results is whether or not the asymptotic parameter R , appearing in the theoretical growth equation quoted earlier in this section, attains a limiting value as general yielding conditions are approached. This was hypothesized to be the case in the Rice, Drugan and Sham study; but the Hermann and Rice data, which actually represent only modest excursions into the general yielding range, tend not to suggest the approach to a limiting R value. Hence one purpose of the continuing experiments will be to provide definitive evidence of this parameter's behavior, and hence assist with the extension of the theory to general yielding conditions.

As mentioned already, the material used for the early experiments, a 4140 steel, was deliberately chosen because it permitted comparison over a wide range of stable crack growth conditions with the theoretical work. Another purpose of the continuing experiments is to now provide data on materials more practical as structural steels. Hence HY 130 is the material currently being tested, and gradually we will move toward lower strength, more ductile materials.

(Staff: R. J. Asaro, W. J. Drugan, L. Hermann, J. R. Rice and T.-L. Sham)

2. Microstructural Aspects of Fracture Processes in Ductile Alloys

a) Void nucleation in spheroidized steels during tensile deformation

While the strengths of many alloy systems are enhanced by the presence of precipitates or dispersed particles, it is observed that these same inhomogeneities act as sites for the initiation of voids during plastic deformation. It is apparent that characterization of the processes by which these voids form in relation to the many parameters which govern the deformation of a particular system is important if the events which lead to the ultimate failure of a material are to be understood and possibly controlled.

For this purpose a systematic study of void nucleation at cementite particles in spheroidized steels during tensile deformation was conducted in an attempt to characterize the nature of the phenomenon in terms of (1) the mode of void formation, (2) location with respect to microstructural features (e.g. particles, grain boundaries), (3) void geometry and (4) material deformation.

An investigation was conducted to determine the effects of various mechanical and material parameters on void formation at cementite particles in axisymmetric tensile specimens of spheroidized plain carbon steels.

Desired microstructures for each of three steel types were obtained by controlled tempering of quenched rods, resulting in various particle size distributions. Cylindrical tensile specimens were then strained to prescribed reductions in the neck area corresponding to deformation levels near fracture.

Observations of void morphology with respect to various microstructural features were made using optical and scanning electron microscopy. While it

was noted that non-equiaxed, irregularly shaped particles often failed by internal fracture, spheroidal particles were observed to form voids by decohesion of the particle-matrix interface in the vicinity of the particle poles. Large particles were favored sites for void nucleation, as were particles situated on ferrite grain boundaries.

The area fraction of voids, f_v, and the number of voids per unit area of transverse cross section, η_A, were measured as functions of deformation in the neck of each specimen.

A criterion for void nucleation based on an analysis of the local stresses and elastic energy storage at spherical particles in a plastically flowing matrix was developed. A critical normal stress requirement and energy balance considerations were incorporated into a double criterion for stable void nucleation:

1) $\sigma_n > \sigma_c$ over the entire interfacial area subject to decohesion (where σ_n is the normal interfacial stress and σ_c is the critical decohesion stress),
2) $\Delta E > \Delta W$ which defines a critical crack size (where ΔE is the combined energy released and ΔW is the energy associated with crack surface formation).

Three-dimensional solutions for the energy release rate associated with polar void cap formation were developed. Contributions to the stored elastic energy in the vicinity of the particles due to applied loading and local plastic incompatibilities were considered and models were evaluated for the present alloy systems in accordance with the proposed nucleation criterion.

The models predict enhanced void nucleation at larger particles and at particles situated on ferrite grain boundaries, consistent with observations.

It was determined that small changes in the work required to form void surfaces can drastically alter the level of deformation necessary for stable void formation.

Effects of non-spherical particle geometries and particle interactions were considered in relation to particle fracture and interfacial decohesion at closely spaced particles.

Good correlation between the computed and measured dependences of void density on deformation was obtained, providing support for the energy analysis used to predict void nucleation. An example is given in Figure 2.1 which shows the variation of hole density as a function of radial distance from the center of the necked portion of the tensile specimens. The triaxial state of stress at the center causes an increase in the number of voids as compared to the material near the surface which is subject to uniaxial stress mainly. This observed effect of stress triaxiality is also predicted by the theory. This part of the work has been completed and is the subject of a Ph.D. thesis by John Fisher (Technical Report No. COO-3084-77).

b) Fracture initiation and propagation in ductile two-phase alloys

As part of a general approach to the fracture of ductile two-phase alloys, several aspects of the interaction of strengthening mechanisms and failure mechanisms were considered.

1) Energy conditions of interfacial void nucleation at iron carbide particles in steels. This problem is described in detail in the preceding section of this report.
2) A comparison of the strength and fracture of two two-phase alloy systems (Technical Report COO-3084-71). The functional

APPLICATION OF HOLE NUCLEATION CRITERION

REFERENCE: JOHN R. FISHER, VOID NUCLEATION IN SPHEROIDIZED STEELS DURING TENSILE DEFORMATION, BROWN UNIVERSITY TECHNICAL REPORT COO-3084-77.

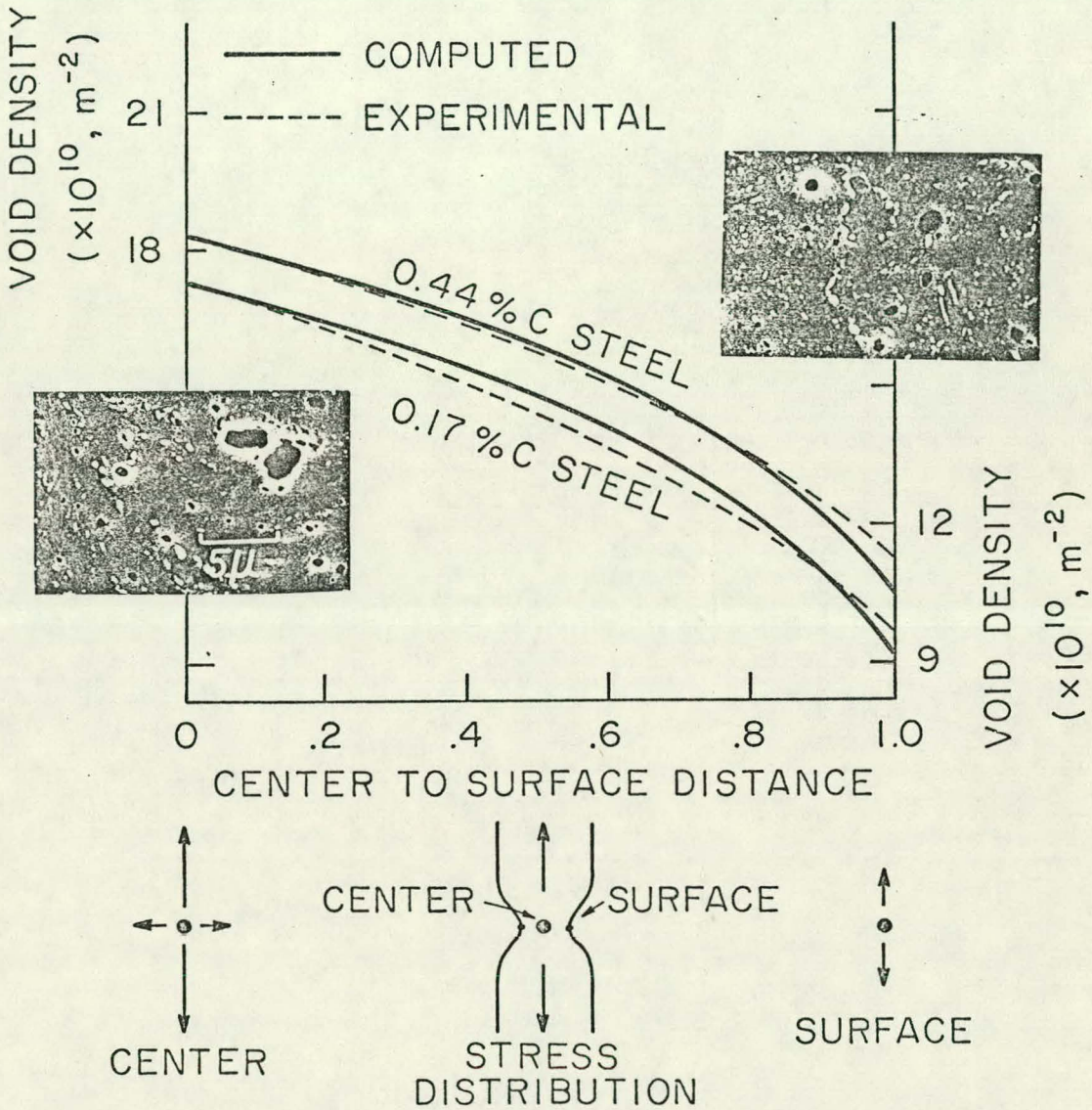

COMPARISON OF THEORETICALLY COMPUTED AND EXPERIMENTALLY MEASURED VOID DENSITIES IN CENTER AND AT SURFACE OF NECKED TENSILE SPECIMENS (THE THEORY PREDICTS AND THE EXPERIMENT CONFIRMS THAT THE NUMBER OF VOIDS PER UNIT AREA IS APPRECIABLY LARGER IN CENTER THAN AT SURFACE DUE TO THE TRIAXIAL STATE OF STRESS AT CENTER OF NECKED PORTION OF TENSILE SPECIMENS. COMPUTED CURVES ARE SCALED TO MATCH THE EXPERIMENTAL CURVES AT CENTER FOR SAKE OF COMPARISON.)

Figure 2.1

roles of the hard and soft constituents in the deformation and fracture of two-phase alloys are discussed on the basis of two commercially important alloy systems, namely, spheroidized carbon steels and cemented carbides, WC-Co . The natures of the two-phases in each alloy are similar, both alloys contain a hard brittle constituent (the carbides FeC or WC) and a soft and ductile constituent (Co or Fe) although in very different relative amounts 5-16% FeC in steel, 65-95% WC in cemented carbides.

On the basis of our past work with both alloys, it is noted that the major stages of the fracture processes in spheroidized steels at low temperatures and in WC-Co alloys at room temperature are similar, in spite of their different microstructures. In both alloys, the initial cracking takes place in the carbide or at the carbide-matrix interface, and is followed by crack growth through the matrix. The ductile fracture process in both alloys may correspond to the fracture model underlying the Rice-Johnson criterion, although the plastic deformation during fracture occurs on very different size scales in the two microstructures, and the fracture toughness values are comparable only within a narrow temperature range. At first glance it may seem surprising that the rather brittle cemented carbide and the more ductile steel are compatible with the same ductile fracture model. However, it should be realized that the materials' fracture behavior was compared only under conditions of small scale yielding. In the case of the spheroidized steel, the small scale yielding condition is obtained only at very low temperatures. In cemented carbides, it holds over a wide range of temperatures (including room temperature) because the extensive plastic

deformation is restricted to the ductile binder phase which constitutes only 5 to 30 volume percent of the alloy. In the case of the cemented carbides, the localized plastic deformation of the binder phase layers at the crack tip contributes the dissipative work, which accounts for most of the fracture energy without greatly affecting the deformation of the bulk of the material which deforms elastically. In both steels and cemented carbides, the linear elastic fracture mechanics are applicable only if the plastic yielding is highly restricted. The conclusions about the fracture process are tentative because the ductile fracture criteria are not yet sufficiently developed to account quantitatively and with confidence for the fracture behavior of a group of alloys over a range of microstructural parameters.

3) The effect of alloy deformation on the average spacing parameters of non-deforming particles (Technical Report C00-3084-75). Since hard particles and crack initiation sites are closely associated, it is of interest to consider whether a geometrical contribution to deformation and fracture could arise from the effect of plastic deformation on particle spacing.

In our analysis, it is shown on the basis of stereological definitions that the commonly used average dispersion parameters, area fraction $(A_A)_\beta$, areal particle density $N_{A\beta}$ and mean free path λ_α, remain invariant during plastic deformation in the case of non-deforming equiaxed particles. Directional effects on the spacing parameters $N_{A\beta}$ and λ_α arise during uniaxial deformation only by rotation and preferred orientation of non-equiaxed particles.

In general, the proper evaluation of the role of particles in deformation and fracture requires careful consideration of the spacing parameters and of their presumed dependence on strain. The above considerations are particularly relevant to the analysis of ductile fracture processes involving particle-nucleated void growth in the necked portion of tensile specimens. In modeling the fracture process it is often assumed that either the particle spacing or the void spacing or both are a geometrical function of strain (for instance, $\lambda_\alpha(\varepsilon) = \lambda_\alpha(0) \exp(-\varepsilon/2)$, where ε is the longitudinal strain and λ_α is the mean free path on a transverse planar section). The assumption derives from theoretical models with parallel cylindrical voids of infinite length, but it has been shown here that it does not generally apply to measures of the average spacing if the particles or holes are appreciably smaller than the specimen or neck length. In the neck, as well as elsewhere in the specimen, the average planar number density of equiaxed particles and the mean free path remain constant with strain and orientation. The planar number density of void intercepts (and their average center-to-center spacing) on a cross-sectional plane is invariant with deformation for longitudinal voids parallel to the tensile specimen axis, unless the volume number density or the longitudinal caliper length of the voids increases with strain, by nucleation of new voids or plastic growth of existing voids, respectively.

4) Deformation and fracture of dual-phase steels. These steels represent a class of alloys which contain massive portions of a hard constituent ($\sim$ 20% martensite) and a soft constituent ($\sim$ 80% ferrite). They are of great current interest to the transportation industry because of the potential weight reduction associated with their use in lieu of the standard

HSLA steels, since they offer improved ductility at comparable strength levels or improved strength at equivalent ductilities. Work has begun on a comparative study of the deformation and failure mechanism in uniaxial tensile deformation and in low cycle fatigue. A preliminary investigation of the dislocation structure development during fatigue was carried out by the graduate student (Andy Szewczyk) during summer work at the research laboratory of the Ford Motor Company, under the supervision of Dr. A. Sherman and Dr. R. G. Davies. An experimental facility to continue this work is being established at Brown.

(Staff: J. Gurland, R. J. Asaro, J. Fisher and A. Szewczyk)

c) Correlation of microstructure with fracture toughness in high strength steels

In our last Progress Report we reported on our work on correlating microstructures in high strength 4140 steels with fracture toughness. The important microstructural features that were controlled were prior austenite grain size, martensite packet size, and carbide size and distribution. Our results for fracture toughness, including plane strain fracture toughness, showed that the prior austenite grain size and the martensite packet size were extremely important for determining toughness, especially plane strain fracture toughness. We found that the results were qualitatively explained quite well using a model fracture criterion which stated that crack advance would take place when the normal strains ahead of the crack tip exceeded a critical amount over a critically large enough distance. This distance is microstructurally significant and was estimated to be linked to the average martensite packet size.

Thus austenitizing at high temperatures, which coarsens the prior austenite grain size and the martensite packet size led to an increased plane strain fracture toughness but to a decreased toughness by all other measures of toughness.

Our new research on 4340 steels is motivated by the previous work on 4140 steel in that we are attempting to control the microstructures and refine particle sizes by austenitizing at high temperatures without producing adversely coarse prior austenite grains. For this purpose we have, in cooperation with Bethlehem Steel Corporation, prepared heats of 4340 which have been grain refined with Aℓ, Zr and Ti. We have found that grain refining with Ti is successful in that we can now maintain grain sizes of less than 60 μm at austenitizing temperatures of 1200 C. By contrast, simple Aℓ killing results in austenite grain sizes of greater than 240 μm at 1200 C. Thus it now appears we are able to carry out our basic plan of varying microstructure, especially particle sizes and spacings, at essentially fixed austenite grain size.

Work has now begun on two heats of steel, an Aℓ-killed and a Ti-Aℓ-killed steel. We are documenting the microstructures and performing plane strain fracture toughness as well as Charpy tests to measure toughness.

(Staff: R. J. Asaro and L. Majno)

3. Environmentally Sensitive Fracture Mechanisms

For the past several years we have conducted research on a number of topics concerned with environmentally sensitive fracture mechanisms. Our recent theoretical work, for example, has been directed at understanding the effect of impurities, including hydrogen, which segregate to internal interfaces, reducing interfacial cohesion and promoting brittle-like separations. Our recent experimental work on the other hand for the past two years or so has been concerned with the role of hydrogen--introduced into the lattices of medium and high strength steels by electrolytic and gas phase charging--in interacting with the normal fracture processes and causing transitions in fracture mode. All these studies have been continued during the past year as outlined below.

a) Thermodynamics of interfacial separation

As an extension of earlier work by Rice and Asaro on the thermodynamics of interfacial separation in the presence of a mobile adsorbed species, Hirth and Rice (Technical Report No. 72) have developed a new presentation of the results in terms of reversible work cycles. Special attention is given to two limiting cases. These are the separation of a material interface under fully equilibrated conditions, for which the chemical potential of the adsorbed solute remains constant, and separation under constrained conditions for which the surface excess solute concentration remains constant (i.e., the same on the two newly created free surfaces as present initially on the unstressed interface). The results are consistent with the limiting cases treated before and include the extension to more general cases of solute interactions, including multi-component systems. The work terms are conveniently represented on diagrams of chemical potential

versus surface excess solute concentration. A general separation process is then represented as a path in this diagram which begins on the adsorption isotherm for the unstressed interface and ends on the adsorption isotherm for the pair of newly created surfaces. This simple graphical presentation makes evident at once the source of difference in work between the two limiting cases and provides a concise means of deriving and summarizing our earlier results on the effects of adsorption on the work of interface separation.

b) The role of hydrogen in medium strength steels

Our previous work conducted on 1045 spheroidized steels showed that hydrogen had an effect on both the initiation and growth of voids. The processes of void initiation, growth and coalescence, though, was not changed from what occurred without hydrogen. Our new work conducted on spheroidized 1017 and 1015 steels has shown similar trends for lower carbon steels as well as some new phenomena which we had not observed in the 1045 steel. Some results on the 1015 steel are discussed below.

When the spheroidized 1015 steel was cathodically charged at current densities less than $2mA/cm^2$ the fracture mode remained ductile and was characterized by void initiation and growth. As in the 1045 steel, hydrogen had the effect of accelerating the void initiation process, causing voids to initiate at lower values of stress or strain. Furthermore, as we reported earlier for the 1045 steel, voids tended to initiate and grow along interfaces, notably grain boundaries, where they coalesced with other voids which grew in a similar manner. However, when the charging current density was increased to $2mA/cm^2$ we observed a progressive transition in fracture mode from ductile void growth and coalescence to transgranular cleavage. This in turn led to a rather large loss in ductility. The portion of the fracture

surfaces characterized by cleavage was found to be a monotonically increasing function of the level of charging current density.

A study was also conducted on the microstructural dependence of the onset of this new fracture mode. Grain size and average particle size were varied as shown in Table 3.1 and results for the "fraction of fracture surfaces characterized by cleavage" versus current density is shown in Fig. 3.1. A preliminary analysis of this data indicates that as the total amount of internal interface (e.g. grain boundary and particle-matrix interfaces) increases, as, for example, in finer grained microstructures or those characterized by finer average particle sizes, there is less tendency to promote cleavage. One possible cause for this behavior is that in coarser microstructures there is much less total sink for hydrogen so that large concentrations can easily develop at inclusions or other interfaces.

We have also indentified some of the specific sites where the observed cleavage initiated--for the most part these were clusters of inclusions of intermetallic compounds of aluminum and manganese. Cleavage facets were larger than any dimension characteristic of the microstructure such as grain size and at present it is not clear what controls the facet size. This is the subject of continuing research.

The results of this study are discussed in detail by Cialone and Asaro in Technical Report No. 78. This report also gives a detailed review of relevant literature on the problem of hydrogen assisted fractures in low and medium strength steels. We have also presented in this report an analysis of void growth by plastic deformation. By using the void growth relations formulated by Rice and Tracy we have shown that the void growth observed in hydrogen charged steels cannot be solely accounted for by the fact that

TABLE 3.1

Microstructural Parameters

Steel	Grain Size	Particle Diameter
A-1015 (tempered 260 hrs)	14 μm	0.9 μm
B-1017 (tempered 24 hrs)	9.0 μm	1.0 μm
C-1017 (tempered 1 hr)	4.2 μm	0.4 μm
D-1017 (thermally cycled 1 hr)	4.4 μm	0.4 μm
E-1017 (austenitized 1 hr at 1323 K, then tempered 1 hr)	11 μm	0.4 μm
1045	4.7 μm	1.0 μm

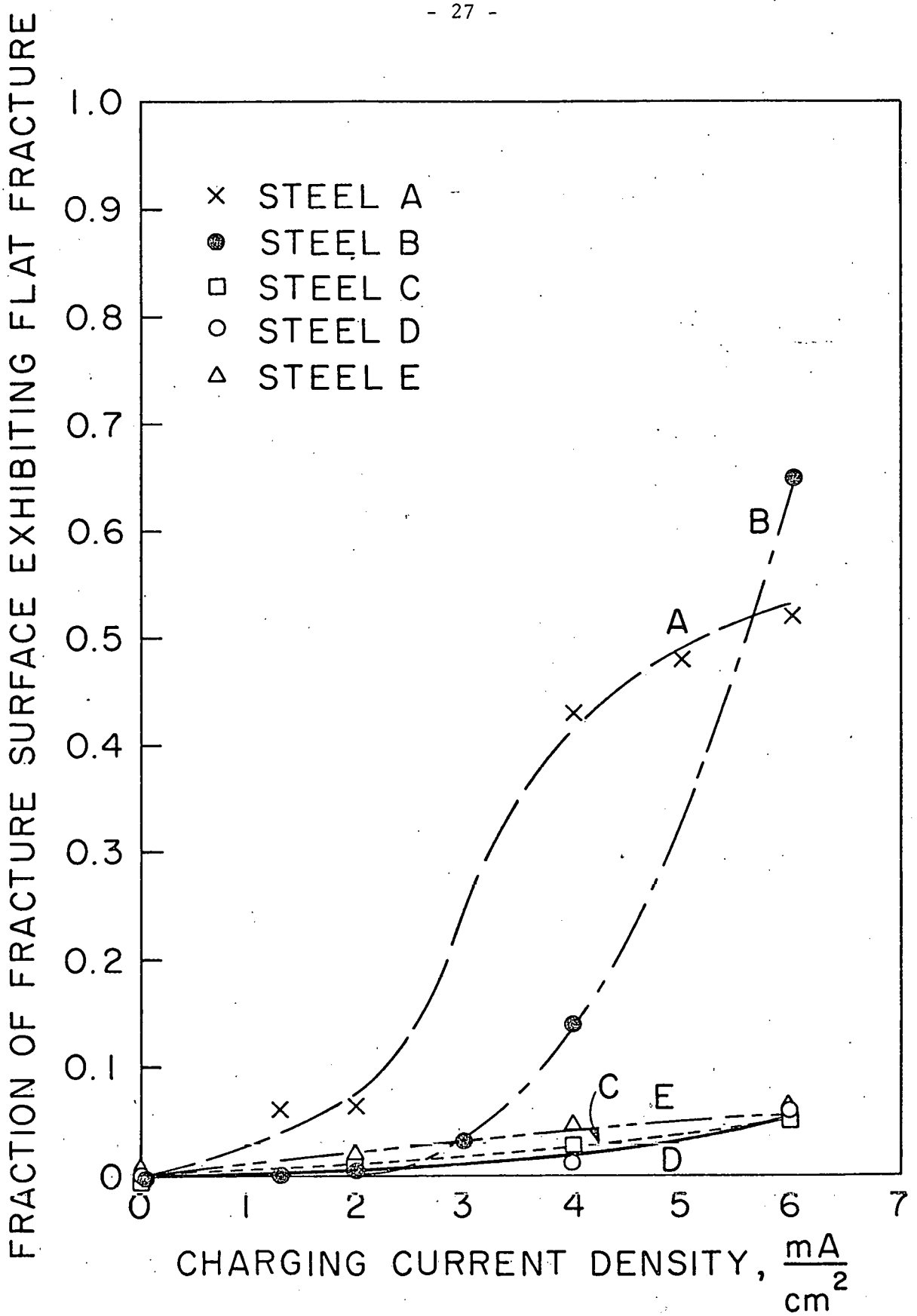
FRACTION OF FRACTURE SURFACE EXHIBITING FLAT FRACTURE
1.0
0.9
0.8
0.7
0.6
0.5
0.4
0.3
0.2
0.1
0
STEEL A
STEEL B
STEEL C
STEEL D
STEEL E
A
B
C
D
E
0
1
2
3
4
5
6
7
CHARGING CURRENT DENSITY, mA/cm²

Figure 3.1

voids initiate sooner (i.e. at smaller strains) with hydrogen than without. This, along with additional metallographic observation, provides further evidence for the idea of hydrogen assisted void growth along interfaces originally discussed by Cialone and Asaro (Met. Trans. 1979, Technical Report No. 59).

c) Hydrogen assisted fractures in high strength steels

Our experimental studies of hydrogen assisted fracture in high strength steels have, to date, focused on the influence of hydrogen on quenched and tempered 4140 steels. We have developed an acoustic emission technique for determining the onset of subsurface fracture induced by hydrogen. In these tests, hydrogen is introduced into the metal through gas phase charging.

By using the acoustical technique described in our last Progress Report we have now identified the metallurgical sites where subsurface cracking initiates as MnS stringers. This has been further verified by performing bend tests on thin wedge loaded specimens (with a configuration similar to compact tension specimens) in a scanning electron microscope. This mode of fracture is not altered with hydrogen, but as in the case of the lower strength steels the critical conditions for fracture are reduced substantially.

Initial tests have been performed on specimens with and without hydrogen. For specimens without hydrogen critical macromechanical conditions for fracture initiation were found by the use of published elastic-plastic analyses of the field near bluntly notched bend specimens. For specimens exposed to one atmosphere of pure hydrogen gas, however, the reduction in the critical bending moment was so large that an elastic solution for the stress field ahead of the notch is now required to estimate the subsurface conditions

needed for crack initiation. We are now conducting a parallel set of experiments on notched and initially smooth tensile specimens with and without hydrogen. The results of these tests will be compared to those of the bend tests.

(Staff: R. J. Asaro, J. R. Rice, H. Cialone)

4. Elevated Temperature Rupture Processes

4a) Processes of diffusive cavitation, including combined effects of plastic creep flow and diffusion

Needleman and Rice have given an analysis of the growth of cavities along grain interfaces by the combined processes of grain boundary diffusion and plastic dislocation creep in the adjoining grains. Their work is reported in Technical Report No. 74, and completes a preliminary analysis by Rice (in "Time Dependent Fracture of Materials at Elevated Temperature", edited by S. Wolf, p. 130, U.S. Department of Energy Report CONF790236 UC-25, Germantown, MD, 1979) which demonstrated the important coupling between plastic creep flow and grain boundary diffusion.

As remarked first by Beere and Speight (Metal Sci., 1978), the coupling between creep and diffusion arises because deformability of the grains allows a localized accommodation of diffused matter near the immediate vicinity of the cavities. As a result, a shorter diffusion path length than that for the rigid-grains model is made possible and hence for a given stress level the cavity growth rate can be increased substantially. A stress and temperature-dependent material length scale L, introduced by Rice, is used to characterize this coupling effect. This is defined by

$$L = (\mathcal{D}\sigma_\infty/\dot{\varepsilon}_\infty)^{1/3}$$

where σ_∞ is the remotely applied equivalent tensile stress, $\dot{\varepsilon}_\infty$ the associated creep strain rate, and $\mathcal{D} = D_b\delta_b\Omega/kT$. Here $D_b\delta_b$ is the grain boundary diffusion coefficient, Ω the atomic volume and kT the energy per atom measure of temperature.

Through this length scale L, one can identify three different regimes of response to the ways in which creep flow can contribute to cavity growth. At large values of a/L, where a is the cavity radius, creep flow alone is important, while diffusion alone dominates the growth

process at small values of a/L . But over a rather broad transition regime (say, $0.2 < a/L < 20$) both mechanisms combine to produce growth in excess (in fact, very much in excess for, say, $1 < a/L < 5$) of growth resulting from either mechanism acting in isolation. Values of L for different metals, based on the recent experimental data of Frost and Ashby (private communication, 1979), have been computed and are tabulated in Technical Report No. 74.

In order to analyze this complicated coupled problem, we established a new variational principle for the combined processes of plastic creep flow and grain boundary diffusion. The principle should be useful for a variety of other creep-diffusion processes (e.g., establishing overall constitutive relations for polycrystals).

The material of the grain is taken as incompressible and non-linear viscous, and is assumed to deform according to

$$\sigma = \Lambda \dot{\varepsilon}^{1/n}$$

in uniaxial tension where Λ and n are constants, and according to

$$\sigma_{ij} - \frac{1}{3}\delta_{ij}\sigma_{kk} = \frac{2}{3}\Lambda \dot{\varepsilon}^{-(n-1)/n}\,\dot{\varepsilon}_{ij}$$

where

$$\dot{\varepsilon} = \sqrt{\frac{2}{3}\,\dot{\varepsilon}_{ij}\,\dot{\varepsilon}_{ij}}\,, \qquad \dot{\varepsilon}_{kk} = 0$$

with

$$2\dot{\varepsilon}_{ij} = \partial v_i/\partial x_j + \partial v_j/\partial x_i$$

for arbitrary stress and strain rate states.

Further, the stresses must satisfy the equilibrium equations

$$\partial\sigma_{ij}/\partial x_i = 0 \quad \text{in} \quad V\,, \qquad n_i\sigma_{ij} = T_j \quad \text{on} \quad S_T$$

where V is the volume occupied by the grains, T_i the surface traction, n_i the unit outward normal to the external boundary, and S_T the portion of that boundary on which tractions are prescribed.

Matter conservation along the grain boundary requires that

$$\partial j_\alpha / \partial x_\alpha + \dot{\delta} = 0$$

where j_α is the volumetric flux crossing unit length in the grain boundary and $\dot{\delta}$ is the rate of opening of one side of the boundary relative to the other. Here α has the range 1, 2 and refers to local Cartesian axes in the plane of the boundary. In addition, the linear isotropic form of the kinetic relation for diffusion is

$$j_\alpha = \mathcal{D} \partial \sigma_n / \partial x_\alpha$$

where σ_n is the normal stress acting on the grain boundary. In typical problems (e.g., cavity growth on a grain boundary) σ_n has some prescribed value, say σ_Ω, where grain boundaries intersect an external (or internal) free surface; σ_o is related to the local curvatures of the free surface at the intersection point.

A new variational principle equivalent to this full set of plastic creep flow and grain boundary diffusion equations is

$$\Delta F = 0 \qquad \text{to first order in} \quad \Delta v_i$$

where

$$F = \int_V \Lambda \frac{n}{1+n} \dot{\varepsilon}^{(1+n)/n} \, dV - \int_{S_T} T_i v_i \, ds + \int_A \frac{1}{2\mathcal{D}} j_\alpha j_\alpha \, dA + \int_\Gamma \sigma_o j_{in} \, d\Gamma \, .$$

Here v_i , j_α and $\dot{\varepsilon}_{ij}$ constitute any kinematically consistent deformation (and associated diffusion flux) field, A denotes the grain boundary area, and Γ denotes the intersections of grain boundaries with free surfaces (with j_{in} being the inwardly-directed diffusive flux along Γ).

Based on this new variational principle, Needleman and Rice formulated finite element equations for the axially symmetric cavity growth model and numerical results were obtained for various values of the parameters a/b , a/L , σ_o/σ_∞ , etc., where 2b is the cavity spacing. From these numerical solutions, cavity growth rate and rupture time (defined here as the time for a cavity to grow from an initial radius a_i to the limiting radius b , at which there is coalescence) were computed. For details of these numerical results, see Technical Report No. 74.

It is found that cavity growth rates are larger than those predicted by the Hull-Rimmer rigid-grains model whenever L is comparable to or smaller than cavity radius a . The values of L computed from experimental data suggest that, e.g., at 0.5 T_m , coupling is important at stresses of the order $10^{-3}\mu$ (μ is the shear modulus) or higher, and unimportant at stresses of the order $10^{-4}\mu$ or lower. L decreases in size with increasing stress and/or temperature.

Beere and Speight (Metal Sci., 1978) and Edward and Ashby (Acta Met., 1979) have proposed a cavity growth model in an attempt to account for the combined effect of creep and diffusion. Their model is based on the concept that each cavity is surrounded by a spherical shell of effectively non-creeping material within which a Hull-Rimmer diffusive cavitation process takes place and these shells are embedded in a matrix of uniformly creeping

material. The patterns of the Mises equivalent shear strain rate distribution, as given by our essentially exact numerical solutions, do not support this concept. However, the simpler models cited do introduce the correct dimensionless parameters (equivalent to L/a and a/b) and predict approximately correct trends.

It is also found that the cavities continue to grow in the presence of overall plastic creep flow even at applied stress levels which are less than the classical sintering limit. The Monkman-Grant product, $\dot{\varepsilon}_{ss} t_r$, where $\dot{\varepsilon}_{ss}$ is the steady state creep strain rate and t_r the rupture time based on growth alone, was computed, and the results show that this product varies with stress level and temperature for a given initial cavity size and half spacing. Evidently, the empirical success of this product cannot be explained on the basis of concepts thus far introduced into theoretical models.

The effect of triaxial stressing on cavity growth for the axially symmetric cavity growth model is now being examined by Needleman and Sham. It is well known that material in front of macro-cracks or notches experiences an elevation in hydrostatic stress. Triaxiality implies an increase in maximum normal stress, which should increase the grain boundary diffusion contribution to growth. Studies on ductile cavity enlargement without diffusion (McClintock, J. Appl. Mech., 1968 and Rice and Tracey, J. Mech. Phys. Solids, 1969) also suggest an effect of triaxiality in accelerating the void growth rate in a manner that depends exponentially on the ratio of remote mean normal stress and yield stress in shear. Our work is examining the interaction of these two mechanisms in the creep range. The finite element program developed by Needleman and Rice for the combined processes of creep

and diffusion is used in this analysis. The problem under study consists of a spherical-caps cavity on a grain boundary at the mid-section of a round bar under triaxial loading.

The work cited thus far has assumed that surface diffusion is rapid enough that a quasi-equilibrium spherical-caps cavity shape is retained; however, the interaction between plastic creep and diffusion leads sometimes to the prediction of such rapid growth rates that this condition will not always be met. Hence, Rice and Sham are studying this effect of non-equilibrium cavity shapes on the cavity growth for the combined processes of creep and diffusion. Work carried out so far has been directed toward determining the cavity profile in the limiting case of rapid growth in the crack-like mode with adjoining grains taken to be deformable. A preliminary study on the cavity profile in the crack-like mode, with the adjoining grains moving apart rigidly with a velocity $\dot{\delta}/2$, has shown that the height $w(r, t)$ of the profile at a distance r from the tip is given by, according to a linearized theory,

$$w(r, t) = [B/v(t)]^{1/3} [\psi - \dot{\delta}/2v(t)] \{1 - \exp [- (a(t) - r)/(B/v(t))^{1/3}]\}$$
$$+ [\dot{\delta}/2v(t)] [a(t) - r]$$

for r near a. Here $B = D_s \delta_s \Omega \gamma_s/kT$, t is the time, ψ is the equilibrium angle at the tip, δ is the effective thickening at the grain boundary due to addition of matter to the adjoining grains, a is the cavity length and $v = \frac{da}{dt}$ is the cavity growth speed. The velocity of the grain, $\dot{\delta}/2$, affects the form of the solution to the profile only through the combination $\dot{\delta}/2v$. It is thought that the same non-dimensional parameter would be important in determining the cavity profile for the general case of deformable

grains. It is because the growth is so rapid that materials near the tip have inadequate time to respond to the overall deformation in the grain and hence these materials move apart rigidly. The investigation on the effect of non-equilibrium shapes is being continued.

As an additional contribution to the understanding of high temperature rupture processes, Rice and Chuang (Technical Report No. 70) have attempted to clarify the procedure of assigning chemical potentials along boundaries (grain boundaries and cavity surfaces) and of calculating energy transfers during diffusive cavity growth. This work was intended to resolve controversies which have arisen in the literature over the circumstances in which elastic strain energy contributions are important, and over the manner in which energy changes associated with cavity growth are to be calculated. For simplicity, in the work it is assumed that the boundaries are flat and that surface and grain-boundary diffusion are the dominant transport mechanisms. As matter diffuses from the void surface into and along the grain boundary, misfit residual stresses are induced to alleviate the high stress concentration ahead of the cavity apex. As a result, it is shown that the contribution of strain energy terms to the chemical potential can be neglected in typical cases. Also, contrary to the Griffith crack extension model, the energy dissipation incurred by diffusive removal of material from the cavity surface and deposition in the grain boundary is a major term in the energy transfers associated with cavity growth. We show that the primary energy "sink" in diffusive cavity growth arises from the work done by the grain-boundary normal stress when matter is inserted in the near-tip region by diffusion, and not from the loss of strain energy of matter that is removed from the cavity at its tip or from a work of bond separation. We also comment on

thermodynamic restrictions on the angle formed by the void surfaces at their apex, where they join the grain boundary. Further, our derivation of boundary values for the chemical potential is carried out in a manner appropriate for arbitrarily large but elastic distortions of material near the cavity tip and, by contrast to most previous work in the area, we include rigorously the effects of surface tension (i.e., of "surface stress", as distinct from surface energy).

(Staff: A. Needleman, J. R. Rice and T.-L. Sham)

4b) Diffusive alleviation of transient stress concentrations

This work investigates the response of partially damaged materials (damage represented as crack-like cavities on grain boundaries) following load or temperature alterations at low stress levels and at temperatures near 0.5 T_m (these conditions are typical in long-term service). Our long-range goals for this area are to examine the effects of non-steady loading (start-up operations, load cycling) on the generation of internal stress concentrations and damage in structural metals and ceramics.

In order to understand the possibilities of the future work on void nucleation and growth under normal operating conditions, we have begun by analyzing the stress field adjacent to pre-existing cavities. We assume that voids were nucleated at some time in the past.

The interaction between grain boundary diffusion and elastic deformation is important at low stress levels (low enough not to produce plastic deformation). The main matter transporting mechanisms are surface and grain boundary diffusion in this case. As discussed by Chuang et al. (Technical Report No. 67 and also Acta Met., 1979), the normal stress, σ, acting on the grain boundary and the effective "thickening", δ, satisfy

$$\mathcal{D} \frac{\partial^2 \sigma}{\partial x^2} + \frac{\partial \delta}{\partial t} = 0 \qquad (1)$$

where t is the time, x is the coordinate directed along the grain boundary and $\mathcal{D} = D_b\delta_b\Omega/kT$. Here $D_b\delta_b$ is the grain boundary diffusion coefficient, Ω is the atomic volume and kT is the energy per atom measure of temperature. We analyze the stress field of a crack-like cavity along a grain boundary under periodic loading which can be represented as a combination of harmonic components. Our solution to this problem can be considered as a first step to analyzing the transient behavior under step loading.

R. Raj (Met. Trans., 1975) and J. R. Weertman (Canadian Met. Qtr., 1979) have analyzed, in an approximate manner, an analogous problem of periodically-distributed voids by treating it as a half-plane problem where the applied stress is approximated by a periodic expansion of the stress distribution acting between cavities. Instead, our analysis is based on the concept of representing a crack as an array of continuously distributed opening dislocations along the grain boundary with a time-dependent dislocation density. In other words, we solve (for simplicity, in the case of plane strain and effectively infinite grain boundary with a cavity between $x = -a$ and $x = +a$) the governing, coupled elasticity and diffusion equations in the form

$$\sigma(x,t) = \sigma_\infty(t) - \frac{E}{4\pi(1-\nu^2)} \int_{-\infty}^{\infty} \frac{\partial\delta(x',t)/\partial x'}{x-x'}\, dx'$$

$$\frac{\partial\delta}{\partial t} + \mathcal{D}\,\frac{\partial^2\sigma}{\partial x^2} = r(x,t)\ . \qquad (2)$$

Here $\sigma_\infty(t)$ is the time-dependent applied stress (in our case state $\sigma_\infty(t) = Ae^{i\omega t}$), $r(x,t)$ is a rate of matter supply, and for simplicity we assume (as did Weertman and Raj) zero stress, σ_o, at the crack tips. Of course, $r(x,t)$ vanishes along the grain boundary outside the cavity. Eliminating δ from these equations, we obtain a representation of the stress distribution as

$$\sigma(x,t) = \sigma_\infty(t) - \frac{E}{4\pi(1-\nu^2)} \int_{-a}^{a} \int_{-\infty}^{t} \frac{\partial r(x',t')/\partial x'}{x-x'} F\left[\frac{\alpha(t-t')}{|x-x'|^3}\right] dt'dx' \qquad (3)$$

where $\alpha = E\,\mathcal{D}/4(1-\nu^2)$ and $[E/4\pi(1-\nu^2)x]F(\alpha t/|x|^3)$ is the solution for the stress distribution along the grain boundary produced by a unit opening dislocation, with core at $x = 0$, suddenly introduced at $t = 0$. This solution has been found in an integral form as

$$F(\alpha t/|x|^3) = \int_0^\infty e^{-u^3 \alpha t/|x|^3} \sin u \, du \, . \qquad (4)$$

From the stress-free boundary condition on the crack surfaces, we obtain the following integral equation (where $R(t,x) = \partial r(t,x)/\partial x$)

$$\sigma_\infty(t) = \frac{E}{4\pi(1-\nu^2)} \int_{-a}^{a} \int_{-\infty}^{t} \frac{R(t',x')}{x'-x} F\left[\frac{\alpha(t-t')}{|x-x'|^3}\right] dt'dx' \qquad (5)$$

for $-a<x<+a$. We seek a solution for cycling load ($\sigma_\infty(t) = \sigma_\infty e^{i\omega t}$) in the form

$$R(t,x) = 4 \frac{\sigma_\infty(1-\nu^2)}{E} P(\omega,x) i\omega e^{i\omega t} \, , \qquad (6)$$

where $P(\omega,x)$ is a complex function and i is the imaginary unit. Substituting this expression for $R(t,x)$ into equation (5) and after performing integration on t', we obtain, after appropriate introduction of dimensionless variables, the integral equation

$$1 = \frac{1}{\pi} \int_{-1}^{1} P(\lambda,y) k(y-x,\lambda) dy \qquad \text{for } -1<x<+1 \, , \qquad (7)$$

where

$$k(y,\lambda) = i\lambda \int_0^\infty \frac{\sin\lambda y v}{i+v^3}\, dv \tag{8}$$

and

$$\lambda = a(\omega/\alpha)^{1/3} = a[4(1-\nu^2)\omega/E\mathcal{D}]^{1/3} . \tag{9}$$

An additional condition on P follows from the symmetry of the problem, i.e., $P(\lambda,y) = -P(\lambda,-y)$. Equation (7) matches well with the linear elastic solution. For $\lambda \to \infty$, $k(y,\lambda) \to 1/y$. For finite λ, $k(y,\lambda)$ is a well-behaved function and we have a Fredholm integral equation of the first kind. There are certain difficulties in solving the equation numerically as can be seen from the following simple consideration. If we substitute in addition to the unknown function an extra term $Ae^{i\gamma y}$, after integration by parts one can find that it is always possible to satisfy the numerical discretization of the integral equation with extra terms of this form. This is a typical indication of an instability effect.

By analyzing the behavior of the kernel, we can find that there is no bounded solution. However, by considering its derivatives (which are also kernels of the integral equations that have to be satisfied by $P(\lambda,y)$), we find that $P(\lambda,y)$ should have a square root singularity at the ends of the interval.

In order to avoid these instability effects, we employ, with some modification, a method developed by A. N. Tikhonov (DAN SSSR, 1963, in Russian). The solution to equation (7) can be obtained by minimizing the following functional:

$$F(f, \frac{\partial f}{\partial x}) = \int_{-1}^{1} \left\{ \left| \frac{1}{\pi} \int_{-1}^{1} P(\lambda,y)k(y-x,\lambda)dy - 1 \right|^2 \right.$$

$$\left. + \frac{\gamma}{\pi\sqrt{1-x^2}} \left[\left| f(\lambda,x) \right|^2 + \left| \frac{\partial f}{\partial x}(\lambda,x) \right|^2 \right] \right\} dx , \tag{10}$$

where $P(\lambda,y) = \dfrac{f(\lambda,y)}{\sqrt{1-y^2}}$ and γ is some small number (like 10^{-8}). Performing variation of the functional F and requiring zero variation at the ends, we obtain an integral equation

$$\frac{1}{\pi}\int_{-1}^{1} \frac{f(\lambda,y)}{\sqrt{1-y^2}} K(x,y)dy + \gamma\left[f(\lambda,x) + \frac{\partial f}{\partial x}(\lambda,x)\right] = \int_{-1}^{1} \overline{k(x,y)}dy \ , \qquad (11)$$

where

$$K(x,y) = \int_{-1}^{1} k(x,z)\overline{k(z,y)}dz \ . \qquad (12)$$

This kernel $K(x,y)$ is smooth and symmetric and we can use the standard collocation scheme to solve this equation. So, the Simpson Rule is used to compute $K(x,y)$ and the integral on the right-hand side of equation (11), and the Chebyshev-Gaussian integration scheme is used to compute the integral on the left-hand side of equation (11). The Chebyshev-Gaussian integration scheme is usually used to obtain numerical solutions to singular integral equations because of the convenience in performing the numerical integration with the weight $1/\sqrt{1-y^2}$. However, in our work, we are interested in stress (or displacement) distributions which are represented by the integrals of the unknown function $f(\lambda,y)$ and which consequently do not depend on the parameter γ as long as it is small and as as long as the resulting solution to the integral equation is stable.

The problem of periodically distributed cracks has been analyzed by a formulation similar to that mentioned above but with a different kernel based on periodically distributed dislocation-like singularities along the grain boundary. We obtain an equation similar to equation (7) with a kernel $k_p(\lambda,y)$ given by

$$k_p(\lambda,y) = \sum_{m=-\infty}^{\infty} k(\lambda, y + 2mb/a) \ , \qquad (13)$$

where $2b$ is the period of the crack distribution.

A numerical solution has been obtained by using the techniques outlined. As can be seen, the solution depends on the parameter λ, linearly on the remotely applied stress σ_∞ (properly non-dimensionalized as $\sigma_\infty^d = \sigma_\infty/[E/4(1-\nu^2)]$), and on the non-dimensionalized crack spacing b/a, where $2b$ is the period.

The remotely applied stress parameter, σ_∞^d, is taken as unity in the plots presented so that the results can be interpreted easily. The parameter λ can be taken as a measure of the effective diffusive region. Specifically, λ as defined in equation (9) is a measure of the ratio of crack half-length, a, to a diffusion penetration distance, $(\alpha/\omega)^{1/3}$, associated with the loading frequency. For $\lambda \gtrsim 1000$, all solutions may be considered as elastic solutions; however, at distances from both crack tips greater than about $10\ a/\lambda$ the stress distribution is very close to the elastic stress distribution for any value of λ.

Typical stress distributions are shown in Fig. 4.1 for values of $\lambda = 5$, 20 and 50, for $b = 2a$. Loading frequencies corresponding to these values of λ are presented in the table for different materials. The table assumes $T = 0.5\ T_m$ and $a = 1\mu m$; the frequencies decrease with decreasing T and with increasing a. Our results differ from those of the approximate solution by J. R. Weertman in the amount of maximum stress, especially at intermediate and large values of λ. This difference is shown in Fig. 4.2 for $\lambda = 20$, $b = 2$.

(Staff: J. R. Rice and A. Rubenstein)

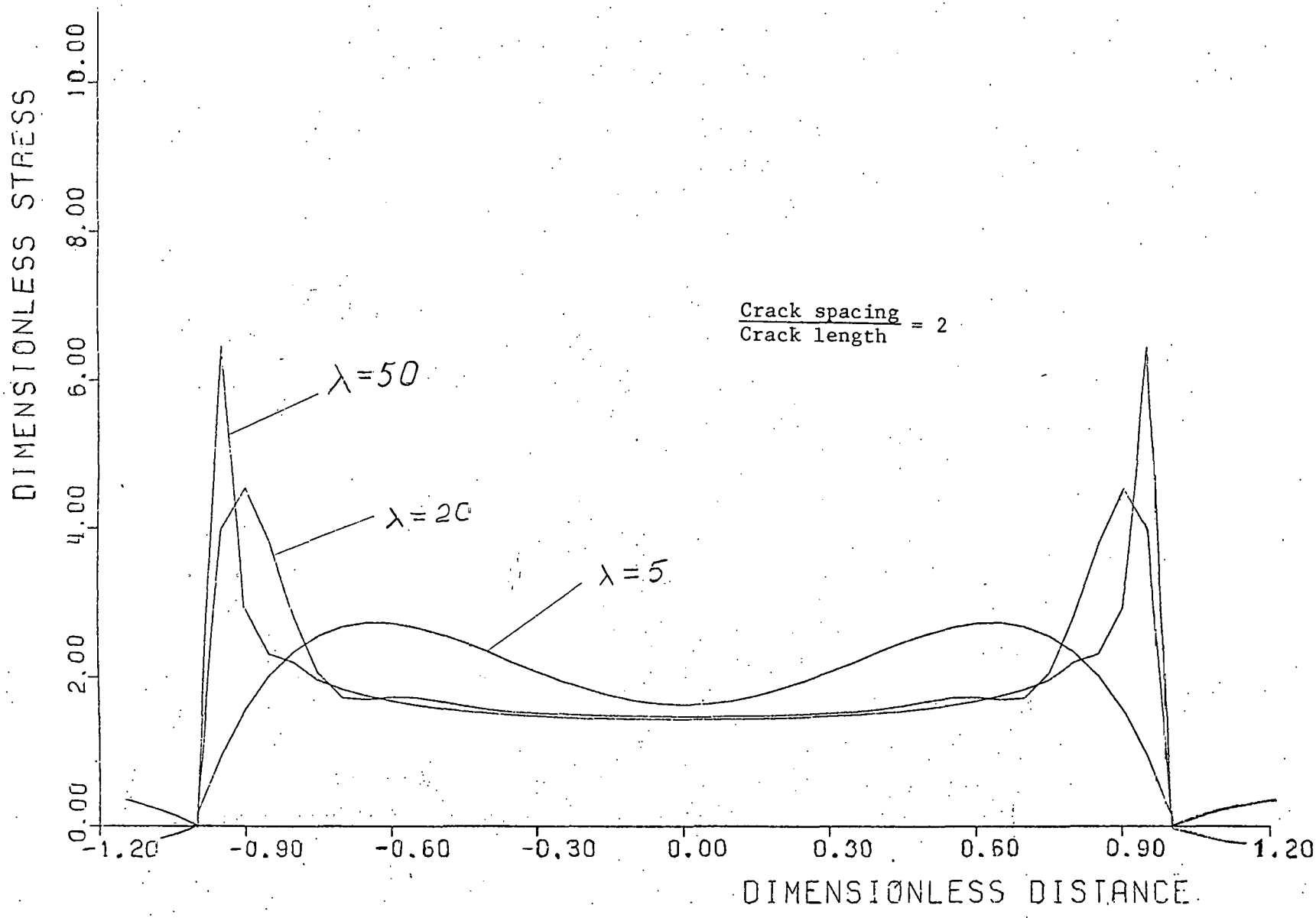

Stress distribution along grain boundary—solutions of the integral equation.

Figure 4.1

Table 4.1

Material	$\frac{\omega}{2\pi}$ (cps) for $\lambda = 5$	$\lambda = 20$	$\lambda = 50$
FCC			
Nickel	0.4	25.5	400.
Copper	0.04	2.52	39.4
Silver	0.09	5.7	90.4
Aluminum	0.02	1.22	19.2
Lead	1.4×10^{-4}	9.1×10^{-3}	0.14
BCC			
Tungsten	5.3×10^{-3}	0.34	5.3
Chromium	2.9×10^{-3}	0.19	2.9
Molybdenum	0.02	1.42	22.2
Alpha Iron	0.1	6.62	103.5
HCP			
Zinc	0.016	1.01	15.9
Magnesium	0.17	11.0	173.

Data for $T = 0.5T_m$ and $a = 1\mu m$

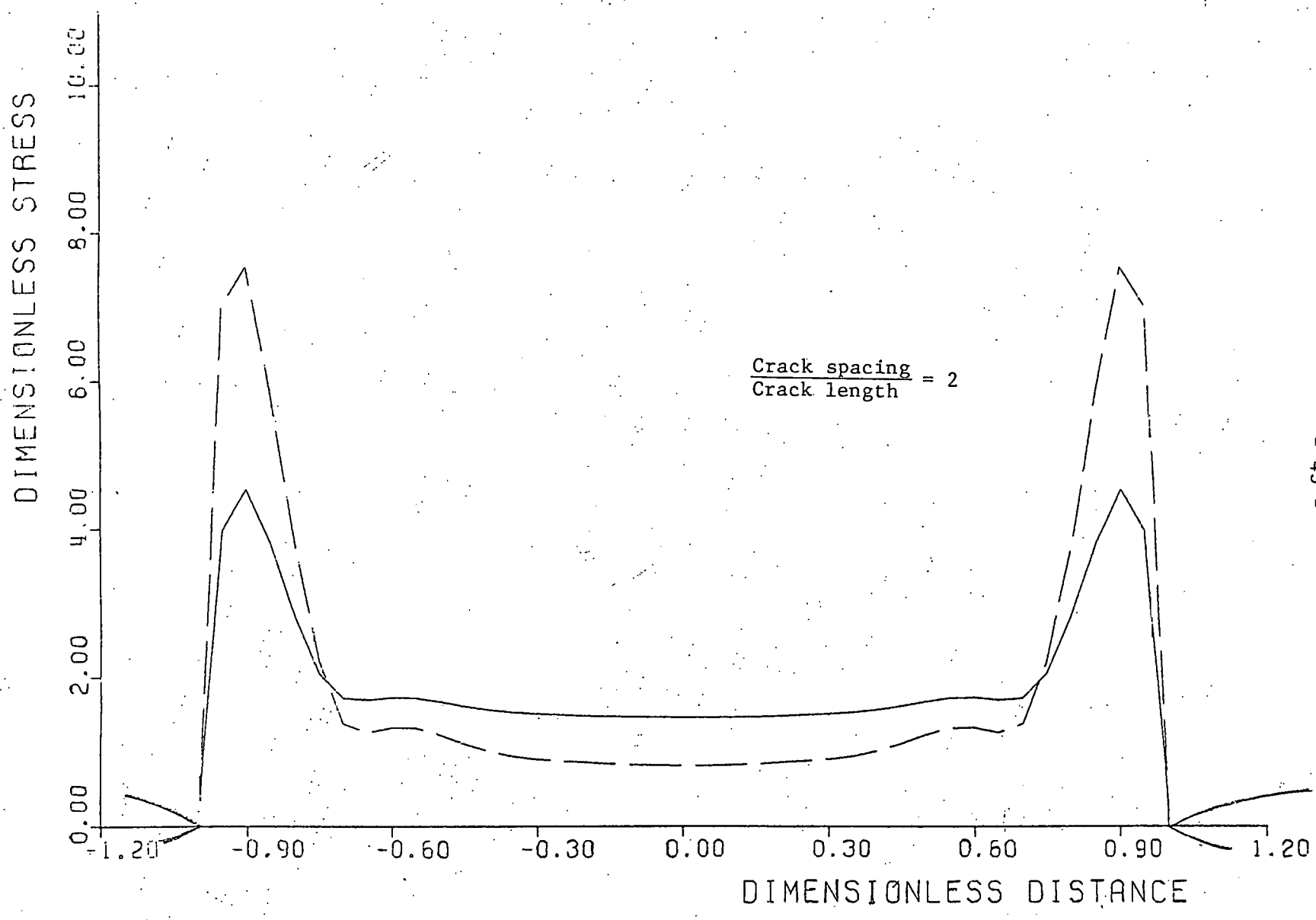

Stress distributions (λ=20); solid line solution of integral equation, dashed line, solution by J.R. Weertman.

Figure 4.2

4c) Creep effects in macro-crack growth

Creep-fatigue interaction is one of the most important problems associated with the failure of structures operating at high stress levels and temperatures. A knowledge of the stress and strain-rate fields in the vicinity of a crack tip is essential to the understanding of the phenomenon of creep-fatigue interaction.

Riedel and Rice (Technical Report No. 64) have analyzed the stress and strain rate fields near a crack tip in an elastic-nonlinear viscous solid subjected to step loading. In their analysis, the material is assumed to obey the elastic-nonlinear viscous relation

$$\dot{\varepsilon}_{ij} = \frac{1+\nu}{E}\dot{\sigma}_{ij} - \frac{\nu}{E}\delta_{ij}\dot{\sigma}_{kk} + \frac{3}{2}B\,\sigma^{n-1}\sigma'_{ij} \quad ,$$

where σ'_{ij} is the deviatoric stress and σ is the equivalent tensile stress

$$\sigma = \sqrt{\frac{3}{2}\sigma'_{ij}\sigma'_{ij}} \quad .$$

Riedel and Rice have shown that the stress and strain rate fields in the vicinity of a stationary crack tip behave, as $r \to 0$, as

$$\sigma_{ij} = \left[\frac{A(t)}{Br}\right]^{1/(1+n)} \Sigma_{ij}(\theta;n)$$

$$\dot{\varepsilon}_{ij} = B\left[\frac{A(t)}{Br}\right]^{n/(1+n)} E_{ij}(\theta;n)$$

where r,θ are polar coordinates about the crack tip, and Σ_{ij}, E_{ij} are functions determined by the analysis (of the same form as Hutchinson-Rice-Rosengren fields for time-independent power-law hardening materials).

They have found that the time-dependent amplitude factor, $A(t)$, approaches the value of the C^*-integral in the long-time limit of steady state creep. For short times after load application, the "small scale yielding" conditions (analogous to those of rate-independent elastic-plastic fracture mechanics) are satisfied and $A(t)$ is given by

$$A(t) \approx K_I^2/[(1+n)Et]$$

for plane stress. A characteristic time, t_1, where

$$t_1 \approx K_I^2/[(1+n)EC^*]$$

was defined on the basis of the short and long time solutions. It represents the transition time from "small scale yielding" to extensive creep. A factor of $1-\nu^2$ must be inserted in the above expressions for plane strain.

Kubo and Rice have used the same assumptions and methods to extend Riedel and Rice's analysis to arbitrary load-varying cases. Based upon the assumption of approximate path-independence of the J-integral, it is found that $A(t)$ is given by

$$A(t) \approx [K_I(t)]^{2(1+n)} \Big/ \left\{(1+n)E \int_o^t [K_I(\tau)]^{2n} d\tau \right\}$$

for plane stress. However, it must be cautioned that the approximations involved become untenable for unloading, so that this analysis does not contribute to understanding typical creep-fatigue effects. A characteristic time, t_1, can also be obtained as the minimum positive root of the following equation:

$$C^*(t_1) = [K_I(t_1)]^{2(1+n)} \Big/ \left\{(1+n)E \int_o^{t_1} [K_I(\tau)]^{2n} d\tau \right\} .$$

In continuing studies, still underway, Kubo is examining the near-tip fields of a stationary crack in solids that obey the Bailey-Orowan type of constitutive relation

$$\dot{\varepsilon}_{ij} = FS^{n-1}(\sigma'_{ij}-\alpha_{ij})$$

$$\dot{\alpha}_{ij} = (C\dot{\varepsilon}_{ij}/\alpha^{\beta}) - D\alpha^{n-\beta-1}\alpha_{ij}$$

where α_{ij} is the "internal stress" parameter, n, β, C, D and F are material constants and α and S are defined as

$$\alpha = \sqrt{\alpha_{ij}\alpha_{ij}}$$

$$S = \sqrt{(\sigma'_{ij} - \alpha_{ij})(\sigma'_{ij} - \alpha_{ij})} \ .$$

This constitutive relation can account for creep recovery which is thought to be one of the causes of high crack growth rates under cyclic or variable loadings at high temperatures. It is found that when steady-state creep conditions are followed by a sudden load change, the Hutchinson-Rice-Rosengren (HRR) singular fields prevail in the vicinity of the crack tip before and after the load change, and that the amplitude of these singular fields can be calculated using material parameters. When $\beta = n-1$, the HRR singular fields are always predominant in the vicinity of the crack tip.

For some ductile materials, creep fracture occurs under steady-state creep conditions. Under these conditions, the HRR singular fields prevail in the vicinity of the crack tip. Kubo has analyzed the problem of Mode I quasi-static crack growth in non-linear viscous materials. In his analysis, the HRR singular fields are combined with a creep damage hypothesis, in which the rate of damage is assumed to be proportional to the b^{th} power

of the equivalent stress. Here b is a temperature-dependent material parameter. Closed form expressions of Mode I crack growth rates are obtained using an approximate method. It is shown that $d\ell/dt$ can be expressed as a power function of the C^*-integral when $b/(n+1)$ is greater than 1. On the contrary, $d\ell/dt$ is dependent on the amount of crack growth as well as the C^*-integral when $b/(n+1)$ is less than 1. However, under usual metallic conditions the effect of the amount of crack growth is thought to be relatively small.

(Staff: S. Kubo and J. R. Rice)

B. Reports, Publications, Theses, Oral Presentations and Other Related Activities

1. Technical Reports

C00-3084-69	Technical Progress Report (June 1979)
C00-3084-70	J. R. Rice and T-j. Chuang, Energy Variations in Diffusive Cavity Growth, (October 1979)
C00-3084-71	J. Gurland, The Strength and Fracture of Two-Phase Alloys - A Comparison of Two Alloy Systems (August 1979)
C00-3084-72	J. P. Hirth and J. R. Rice, On the Thermodynamics of Adsorption at Interfaces as it Influences Decohesion (October 1979)
C00-3084-73	Final Report (November 1979)
C00-3084-74	A. Needleman and J. R. Rice, Plastic Creep Flow Effects in the Diffusive Cavitation of Grain Boundaries (February 1980)
C00-3084-75	J. R. Fisher and J. Gurland, The Effect of Alloy Deformation on the Average Spacing Parameters of Particles (February 1980)
C00-3084-76	L. Hermann and J. R. Rice, Comparison of Experiment and Theory for Elastic-Plastic Plane Strain Crack Growth (March 1980)
C00-3084-77	J. R. Fisher, Void Nucleation in Spheroidized Steels During Tensile Deformation (April 1980)
C00-3084-78	H. Cialone and R. J. Asaro, Hydrogen Assisted Fracture of Spheroidized Plain Carbon Steels (June 1980)

2. Publications

*R. J. Asaro, "Adsorption Induced Losses in Interfacial Cohesion", Phil. Trans. Roy. Soc. London A295, 151 (1980).

H. Cialone and R. J. Asaso, "Hydrogen Assisted Fracture of Spheroidized Plain Carbon Steels", to appear in Proc. of Third International Conference on Effect of Hydrogen on Behavior of Materials.

J. Gurland, "An Approximate Method for the Estimate of the Contribution of Load Transfer to the Internal Stress in Dispersed Particles", Scripta Metallurgica 13 (1979), p. 967.

J. Gurland, "The Strength and Fracture of Two-Phase Alloys - A Comparison of Two Alloy Systems", in Fracture '79, Proceedings of the Conference on Fracture, University of the Witwatersrand, Johannesburg, South Africa, 1979, p. 69.

* Listed as "in press" or "submitted" in last year's progress report.

J. R. Fisher and J. Gurland, "The Effect of Alloy Deformation on the Average Spacing Parameters of Non-Deforming Particles" (submitted to Metallurgical Transactions)

*H. Riedel and J. R. Rice, "Tensile Cracks in Creeping Solids", ASTM-STP, in press.

*J. R. Rice, W. J. Drugan and T.-L. Sham, "Elastic Plastic Analysis of Growing Cracks", ASTM-STP, in press.

A. Needleman and J. R. Rice, "Plastic Creep Flow Effects in the Diffusive Cavitation of Grain Boundaries", Acta Met., in press (as Overview Paper).

J. R. Rice and T.-j. Chuang, "Energy Variations in Diffusive Cavity Growth", J. Amer. Ceramic Soc., in press.

L. Hermann and J. R. Rice, "Comparison of Experiment and Theory for Elastic-Plastic Plane Strain Crack Growth", Metal Sci., in press.

J. P. Hirth and J. R. Rice, "On the Thermodynamics of Adsorption at Interfaces as it Influences Decohesion", Metallurgical Trans., in press.

3. Thesis

J. R. Fisher, Ph.D., June 1980, "Void Nucleation in Spheroidized Steels During Tensile Deformation"

4. Oral Presentations and Seminars

W. J. Drugan

M.I.T., Solid Mechanics Seminar, October 1979, "Elastic-Plastic Crack Growth in Ductile Solids"

J. R. Fisher

Presentations on fracture of steel at General Motors Company, Research Laboratory, Detroit, MI; Kennametal, Inc., Greensburg, PA; and Western Electric Company, Engineering Research Center, Princeton, NJ.

J. Gurland

Ford Motor Company Research Laboratory, Dearborn, MI, June 1979;
Keynote speaker and lecturer, at Fracture '79, University of the Witwatersrand, Johannesburg, South Africa, November 1979;
Center for Scientific and Industrial Research (CSIR), Pretoria, South Africa, November 1979.
Boart Hard Metals, Ltd., Springs, South Africa, November 1979.

J. R. Rice

M.I.T., Materials Science Colloquium, Dec. 1979, "Elevated Temperature Diffusive Cavitation of Grain Boundaries";
AIME Symposium on Microstructure and Fracture of High Toughness Alloys (Las Vegas), Feb. 1980, "Elastic-Plastic Crack Growth";
British Metals Soc./Inst. Physics Conference on Micromechanics of Fracture (Cambridge, England), March 1980, "Comparison of Experiment and Theory for Elastic-Plastic Plane Strain Crack Growth";
National Bureau of Standards, Materials Seminar, February 1980, "Elevated Temperature Diffusive Cavitation of Grain Boundaries";
IUTAM Symposium in Three Dimensional Constitutive Relations and Ductile Rupture (Dourdan, France), June 1980, "Processes of Plastic Cavity Growth";
Polish Academy of Sciences, Short Course on Materials Damage and Fracture (Warsaw, Poland), June 1980: Various lectures on elastic-plastic fracture mechanics and processes of ductile cavitation.

A. Needleman

16th Annual Meeting of the Society for Engineering Science (Evanston, IL) September 1979;
M.I.T. Solid Mechanics Seminar, November 1979;
ASTM Task Force Meeting on High Temperature Fracture Processes (Cambridge, Mass.), December 1979: "Diffusive Growth of Grain Boundary Voids in Creeping Solids".

R. J. Asaro

IUTAM Symposium, Dourdan, France, June 1980, "Some Effects of Hydrogen on Void Initiation and Ductile Fracture".

S. Kubo

Brown University, April 1980, "Phenomenological Analysis of Creep Crack Propagation in Ductile Materials".

C. Personnel

1. Professional Staff: R. J. Asaro, J. Gurland, A. Needleman and J. R. Rice.
2. Research Engineer: L. Hermann.
3. Technical Assistants: W. Rebello and H. Stanton.
4. Research Assistants (Graduate Students): H. Cialone, W. J. Drugan, J. R. Fisher, L. Majno, A. Rubenstein, *A. Szewcyzk and *T-L. Sham.
5. Visiting Research Associates: **Dr. Len Simpson and Dr. S. Kubo.
6. Senior Undergraduate Research Assistants: Joseph Anastasio, Elizabeth Brisbin and Simon Tse.

*Supported for portion only of contract period.

**Not supported by contract.